STRESS-STRAIN MODEL FOR FERRITIC STAINLESS STEELS

ZHONG TAO
KIM RASMUSSEN

RESEARCH REPORT R953
APRIL 2015
ISSN 1833-2781

SCHOOL OF CIVIL ENGINEERING

THE UNIVERSITY OF SYDNEY

THE UNIVERSITY OF SYDNEY

SCHOOL OF CIVIL ENGINEERING

STRESS-STRAIN MODEL FOR FERRITIC STAINLESS STEELS

RESEARCH REPORT R953

ZHONG TAO
KIM RASMUSSEN

April 2015

ISSN 1833-2781

Copyright Notice

School of Civil Engineering, Research Report R953
Stress–Strain Model for Ferritic Stainless Steels
Zhong Tao
Kim Rasmussen
April 2015

ISSN 1833-2781

Published by:
School of Civil Engineering
The University of Sydney
Sydney NSW 2006
Australia

This report and other Research Reports published by the School of Civil Engineering are available at http://sydney.edu.au/civil

ABSTRACT

Compared with austenitic or duplex stainless steels, ferritic stainless steels have no or very low nickel content. Therefore, their cost is lower and more stable than those of austenitic and duplex stainless steels, providing a more viable alternative for structural applications. Existing stress–strain models, however, are less accurate in predicting stress–strain curves of ferritic stainless steels than for austenitic and duplex stainless steels, since ferritic stainless steels behave more similarly to plain carbon steel. A wide range of tensile test data were collected for ferritic stainless steel coupons, either cut from steel sheets or cold-formed hollow sections. Using the three basic Ramberg-Osgood parameters, stress–strain models are developed for both flat and corner ferritic stainless steels. The accuracy of the proposed models is verified by comparing their predictions with experimental stress–strain curves.

KEYWORDS

Stainless steel; Ferritic stainless steel; Stress–strain relation; Cold-formed; Corner effects.

TABLE OF CONTENTS

INTRODUCTION

Compared with other types of stainless steels, martensitic alloys generally have lower weldability, ductility and corrosion resistance, and are more susceptible to stress corrosion cracking. Therefore, only austenitic, duplex and ferritic steels are recommended in EN 1993-1-4 (2006) for structural applications. Nowadays, the structural use of stainless steel is of increasing interest to engineers due to the benefits which stainless steel can offer. But such structural applications have been greatly inhibited by the high initial material cost (Gardner 2008; Uy et al. 2011). Compared with austenitic or duplex stainless steels, ferritic stainless steels normally contain much lower nickel. Therefore, their cost is lower and more stable than those of austenitic and duplex stainless steels, providing a more viable alternative for structural applications (Afshan and Gardner 2013). Ferritic stainless steels predominantly consist of iron and chromium, and share the same body-centred cubic structure as pure iron (Hedström 2007). On the other hand, austenitic stainless steels have a face-centred cubic crystal structure with sufficient nickel and/or manganese content to retain this austenitic structure at room temperature, whereas duplex stainless steels have a mixed microstructure of austenite and ferrite. Due to the difference in chemical composition and microstructure, it is expected that ferritic stainless steels have different mechanical behaviour compared with other stainless steels. In general, ferritic stainless steels are more similar in their mechanical behaviour to carbon steel (McGuire 2008).

A number of stress (σ)–strain (ε) models proposed by Rasmussen (2003), Gardner and Nethercot (2004), and Quach et al. (2008) are available for stainless steels at room temperature. The stress–strain behaviour of stainless steels is modeled in either two stages or three stages. In general, there is no significant difference among the three model predictions up to strains of general structural interest (Tao et al. 2011), and Rasmussen's two-stage model (Rasmussen 2003) is the simplest to use and is adopted in EN 1993-1-4 (2006).

Cold-forming involves coiling, uncoiling and leveling processes before roll forming or press braking, and has a significant influence on the σ–ε curves of stainless steels (Afshan 2013). Wang et al. (2014) proposed a σ–ε model for stainless steel in the corner regions of cold-formed hollow sections to address the so-called cold-forming effect. That model was specifically proposed for austenitic and duplex stainless steels, rather than for ferritic stainless steels.

All aforementioned σ–ε models have been less exhaustedly verified for ferritic stainless steels compared to austenitic and duplex alloys due to the lack of test data in the past. Nowadays, a wide range of test data for ferritic stainless steels is available due to the increasing research interest in this alloy type. There is a need to use this data to check the applicability of the existing σ–ε models for ferritic stainless steels. In this paper, an extensive survey of the literature is conducted to collect tensile test data of ferritic stainless steels. Stress–strain models are developed for both flat material and corner material in cold-formed ferritic stainless steel hollow sections. The experimental stress–strain curves are used to verify the accuracy of the proposed models.

TEST DATA AND MODEL EVALUATION

TEST DATA

A wide range of tensile test data are collected for seven ferritic stainless steel grades: 1.4003 (S40977), 1.4016 (S43000), 1.4509 (S43932), 1.4512 (S40900), 1.4521 (S44400), 1.4621 (S44500) and 1.4622 (S44330), where the unbracketed and bracketed grades are designations according to EN 10088-1 (2005) and the Unified Numbering System (ASTM International 2012), respectively. The test data is for coupons cut either from steel sheets or hollow sections. A total of 95 tests including 35 full-range σ–ε curves for steel sheets and flat regions of square hollow sections (SHS) or rectangular hollow sections (RHS) are collected from 21 studies presented by van der Merwe et al. (1986), van der Merwe and van den Berg (1987), Hyttinen (1994), Bredenkamp and van den Berg (1995), Korvink et al. (1995), Oliphant et al. (2000), Lecce and Rasmussen (2005), Rossi (2008), Becque and Rasmussen (2009a; 2009b), Islam and Young (2012), Real et al. (2012), Cashell (2012), Manninen (2013), Afshan and Gardner (2013), Afshan et al. (2013), Arrayago et al. (2013), Lim et al. (2013), Rossi et al. (2013), Dundu and van Tonder (2014) and Niu et al. (2014). In the following, both material cut from steel sheets and that in the flat regions of hollow sections are referred to as ″flat material″ since a same σ–ε model can normally be used for them. The literature review indicates that less studies were conducted for corners cut from hollow sections, where a total of 10 tests with full-range σ–ε

curves were reported by Hyttinen (1994), Afshan and Gardner (2013) and Afshan et al. (2013). For simplicity, the material in the corners is referred to as ″corner material″ hereafter. The details of the test data for flat and corner material are summarised in Tables 1 and 2. For flat material, the yield stress determined by the 0.2% proof stress (f_y) ranges from 257 to 536 MPa, whereas the range of the ultimate tensile strength (f_u) is from 421 to 576 MPa. For corner material, the strength enhancement in f_y ranges from 5 to 26%, and that in f_u ranges from 8 to 26%.

Table 1. Summary of Test Data for Flat Material

Source	Steel grade	Number of specimens	Number of curves	E_0 (GPa)	n	f_y (MPa)	f_u (MPa)	Product
van der Merwe et al. (1986)	1.4003	4	–	196–230	8–14	307–353	480–506	Sheet
van der Merwe and van den Berg (1987)	1.4016	8	–	195–222	8–22	304–366	510–562	Sheet
Hyttinen (1994)	1.4003	5	3	205–213	4–7	340–536	497–576	Sheet, SHS
	1.4512	5	3	204–208	7–20	257–498	421–513	Sheet, SHS
Bredenkamp and van den Berg (1995)	1.4003	6	–	194–225	–	337–393	453–542	Sheet
Korvink et al. (1995)	1.4003	2	–	188–220	–	277–302	471	Sheet
	1.4016	2		190–213		308–334	492	Sheet
Oliphant et al. (2000)	1.4003	2	–	171–192	–	314–345	525–549	Sheet
Becque and Rasmussen (2009a) [a]	1.4003	4	1	199–220	6–10	328–378	443–489	Sheet
	1.4016	4	–	192–213	7–13	280–309	431–460	Sheet
Becque and Rasmussen (2009b)	1.4521	2	–	201–216	12–23	302–310	450–451	Sheet
Rossi (2008)	1.4003	3	–	176–183	11–15	314–346	448–471	Sheet
Islam and Young (2012)	1.4003	5	–	199–204	5–6	426–504	446–514	SHS, RHS
Manninen (2013)	1.4003	1	1	194	9	330	493	Sheet
	1.4016	3	3	175–199	8–11	311–338	458–478	Sheet
	1.4509	3	3	195–204	10–12	331–440	479–524	Sheet
	1.4521	2	2	192–195	12	375–394	542–564	Sheet
	1.4621	1	1	184	12	359	469	Sheet
Real et al. (2012) [b]	1.4003	3	3	191–220	6–8	328–330	479–480	Sheet
	1.4016	6	1	167–196	8–14	309–317	444–467	Sheet
	1.4509	6	1	191–207	10–16	331–368	464–472	Sheet
	1.4521	3	1	197–205	9–12	392–394	539–551	Sheet
Afshan and Gardner (2013)	1.4003	3	3	210–219	8–10	423–454	447–475	SHS, RHS
	1.4509	1	1	218	8	519	534	SHS
Afshan et al. (2013) [c]	1.4003	2	2	190–197	8–11	426–439	469–470	SHS, RHS
	1.4509	3	3	190–196	7	466–507	515–536	SHS
Arrayago et al. (2013)	1.4016	1	1	213	11	316	502	Sheet
Lim et al. (2013)	1.4016	1	1	165	–	317	435	Sheet
Rossi et al. (2013)	1.4003	2	–	–	–	437–459	490–505	SHS, RHS
Dundu and van Tonder (2014)	1.4003	1	–	193	–	280	469	Sheet
Niu et al. (2014)	1.4622	1	1	202	13	288	428	Sheet

[a] Full-range curves reported by Lecce and Rasmussen (2005).
[b] Full-range curves presented by Cashell (2012).
[c] Full-range curves provided in private correspondence.

Statistical analysis of the test data indicates that ferritic stainless steel demonstrates obvious anisotropic behaviour. The values of E_0, f_y and f_u for test coupons aligned parallel to the rolling direction are generally lower than those in transverse or diagonal directions (Hyttinen 1994; Bredenkamp and van den Berg 1995; Korvink et al. 1995; Oliphant et al. 2000; Lecce and Rasmussen 2005; Rossi 2008; Becque and Rasmussen

2009a, 2009b; Niu et al., 2014), where E_0 is the initial elastic modulus. The average anisotropy ratios and standard deviations (SD) for E_0, f_y and f_u are presented in Table 3, which particularly highlights the marked anisotropy for E_0 and f_y. However, for the strain-hardening exponent *n*, no clear trend in anisotropy can be observed due to the scarcity of test data and the significant variation.

Table 2. Summary of Test Data for Corner Material

Source	Steel grade	Number of specimens	Number of curves	$E_{0,c}$ (GPa)	n_c	$f_{y,c}$ (MPa)	$f_{u,c}$ (MPa)
Hyttinen (1994)	1.4003	2	2	199–265	3	526–558	612–628
	1.4512	2	2	187–258	5–6	500–521	524–554
Afshan and Gardner (2013)	1.4003	3	3	200–226	5–8	512–545	520–597
	1.4509	1	1	225	4	580	665
Afshan et al. (2013) [a)]	1.4003	2	2	201–210	6–11	518–530	539–551

[a)] Full-range curves provided in private correspondence.

Table 3. Statistical Summary of Anisotropy Ratios

Angle to the rolling direction	Number of test data	Ratio for E_0		Ratio for f_y		Ratio for f_u	
		Mean	SD	Mean	SD	Mean	SD
30	2	1.070	0.020	1.036	0.004	0.980	0.067
45	4	1.061	0.039	1.083	0.025	1.026	0.041
90	23	1.104	0.037	1.088	0.036	1.048	0.034
In total	**29**	**1.095**	**0.039**	**1.084**	**0.036**	**1.039**	**0.040**

Nominal values of E_0, f_y, f_u and *n* are provided in EN 1993-1-4 (2006) for ferritic grades 1.4003, 1.4016 and 1.4512. No specifications, however, are given for other ferritic grades in EN 1993-1-4 (2006). To provide information for engineers, the average measured values and standard deviations of different parameters are presented in Table 4 for different ferritic grades (flat material in longitudinal tension only). The normal range of chromium content specified in ASTM International (2012) is also presented for each ferritic grade. As can be seen from Table 4, the average measured values of E_0 for all grades are quite close to 200,000 MPa, which is also the value of elastic modulus normally specified for carbon steel. But the nominal value of E_0 given in EN 1993-1-4 (2006) is 220,000 MPa for ferritic stainless steels, which is higher than that specified for other stainless steels. This is not supported by the current statistical analysis. Meanwhile, it is found that the specified values of f_y and f_u in EN 1993-1-4 (2006) are much lower than the average measured values presented in Table 4. For f_y of ferritic grades 1.4003, 1.4016 and 1.4512, the average measured values are

Table 4. Statistical Summary of Mechanical Properties for All Flat Material

Steel grade	Chromium content (%)	Number of test data	E_0 (MPa)		*n*		f_y (MPa)		f_u (MPa)	
			Mean	SD	Mean	SD	Mean	SD	Mean	SD
1.4003	10.5-12.5	31	201,400	13,000	8	2.5	385	71.8	485	28.2
1.4016	16-18	21	194,600	16,400	11	3.3	321	19.8	489	42.0
1.4509	17-19	12	199,600	7,900	10	2.6	402	73.4	493	29.3
1.4512	10.5-11.75	3	206,300	2,100	11	7.5	420	106.0	473	47.3
1.4521	17.5-19.5	6	197,900	4,500	11	1.3	375	36.5	533	41.4
1.4621	19-21	1	184,000	–	12	–	359	–	469	–
1.4622	18-23	1	201,500	–	13	–	288	–	428	–
In total		**75**	**198,900**	**12,700**	**10**	**3.2**	**369**	**67.4**	**490**	**36.5**

33-100% higher than the specified nominal values, whereas the average measured values of f_u are 9-25% higher than the specified nominal f_u. For the *n*-values in the longitudinal direction, the specified *n*-values are 16-78% lower than the average measured *n*.

It is worth noting that the nominal values specified in EN 1993-1-4 (2006) are for annealed steel sheets, but the average measured values shown in Table 4 are for specimens of both steel sheets and flat regions of cold-formed hollow sections. The latter might have experienced work hardening in the forming process. Table 5 shows the average measured values and standard deviations of different parameters for different ferritic grades after excluding the test data for hollow sections. Even in this case, the average measured values of f_y are still 16.7-42.3% higher than the specified nominal values in EN 1993-1-4 (2006) and the average measured values of f_u are 7.6-10.8% higher than the specified nominal f_u. This comparison indicates that the suitability of the nominal values specified in EN 1993-1-4 (2006) may need to be reassessed for ferritic stainless steels.

Table 5. Statistical Summary of Mechanical Properties for Steel Sheets only

Steel grade	Chromium content (%)	Number of test data	E_0 (MPa)		n		f_y (MPa)		f_u (MPa)	
			Mean	SD	Mean	SD	Mean	SD	Mean	SD
1.4003	10.5-12.5	17	198,400	15,500	9	2.6	327	24.6	484	18.9
1.4016	16-18	21	194,600	16,400	11	3.3	321	19.8	489	42.0
1.4509	17-19	9	200,100	5,000	11	2.0	359	35.3	477	19.3
1.4512	10.5-11.75	1	207,000	–	20	–	299	–	421	–
1.4521	17.5-19.5	6	197,900	4,500	11	1.3	375	36.5	533	41.4
1.4621	19-21	1	184,000	–	12	–	359	–	469	–
1.4622	18-23	1	201,500	–	13	–	288	–	428	–
In total		**56**	**197,300**	**13,200**	**11**	**3.0**	**335**	**32.5**	**488**	**37.0**

EVALUATION OF RASMUSSEN'S MODEL

Rasmussen's model (Rasmussen 2003) has been included in EN 1993-1-4 (2006) and widely used by other researchers. It is a two-stage σ–ε model using only three basic Ramberg–Osgood parameters (E_0, f_y, and n), where the strain-hardening exponent n is determined by f_y and the 0.01% proof stress $f_{0.01}$:

$$n = \frac{\ln(20)}{\ln(f_y / f_{0.01})} \tag{1}$$

The σ–ε relationship proposed by Rasmussen (2003) is as follows:

$$\varepsilon = \begin{cases} \dfrac{\sigma}{E_0} + 0.002\left(\dfrac{\sigma}{f_y}\right)^n & \text{for} \quad \sigma \le f_y \\ 0.002 + \dfrac{f_y}{E_0} + \dfrac{\sigma - f_y}{E_y} + \varepsilon_u\left(\dfrac{\sigma - f_y}{f_u - f_y}\right)^m & \text{for} \quad f_y < \sigma \le f_u \end{cases} \tag{2}$$

where E_y is the tangent modulus of the σ–ε curve at the yield stress, and m is a coefficient determining the shape of the second stage of the curve. E_y and m can be calculated by Eqs. (3) and (4), respectively. Meanwhile, Eqs. (5) and (6) were proposed by Rasmussen (2003) to determine f_u and the related ultimate strain ε_u. It should be noted that Eq. (5) was proposed for all alloys, and the predictions have greater scatter compared to the predictions using another equation specifically proposed for austenitic and duplex stainless steels by Rasmussen (2003).

$$E_y = \frac{E_0}{1 + 0.002nE_0 / f_y} \tag{3}$$

$$m = 1 + 3.5\frac{f_y}{f_u} \tag{4}$$

$$\frac{f_y}{f_u} = \frac{0.2 + 185 f_y / E_0}{1 - 0.0375(n-5)} \tag{5}$$

$$\varepsilon_u = 1 - \frac{f_y}{f_u} \tag{6}$$

Although extensive test data has been used by Rasmussen to verify his model (Rasmussen 2001), the majority of the test data was for austenitic and duplex stainless steels. In contrast, only 12 test data of ferritic stainless steels reported by van der Merwe et al. (1986) and van der Merwe and van den Berg (1987) were used, where the yield stress ranged only from 304 to 366 MPa. To further verify the accuracy of Rasmussen's model in predicting σ–ε curves of ferritic stainless steels, the test data summarised in Table 1 for ferritic stainless steels is used in this paper. Figure 1 shows the prediction accuracy of f_u using Eq. (5) proposed by Rasmussen (2003). In general, f_u is overpredicted, and the overprediction can be over 30% when f_u is greater than 400 MPa. Meanwhile, f_u is significantly underpredicted for a few specimens with an *n*-value greater than 14. This is owing to the fact that the predicted f_u from Eq. (5) is very sensitive to the *n*-value, which in turn greatly affects the predicted ε_u and σ–ε curve, as shown in Fig. 2. According to the test data collected, the measured *n*-values for ferritic stainless steels range from 4.2 to 22.5, which demonstrate significant variation. It is also found that ε_u of ferritic stainless steels is overpredicted by using Eq. (6).

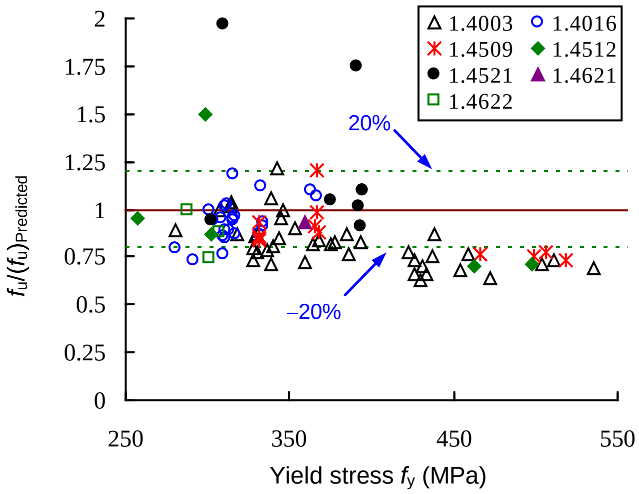

Fig. 1. Prediction accuracy of f_u using Rasmussen's model

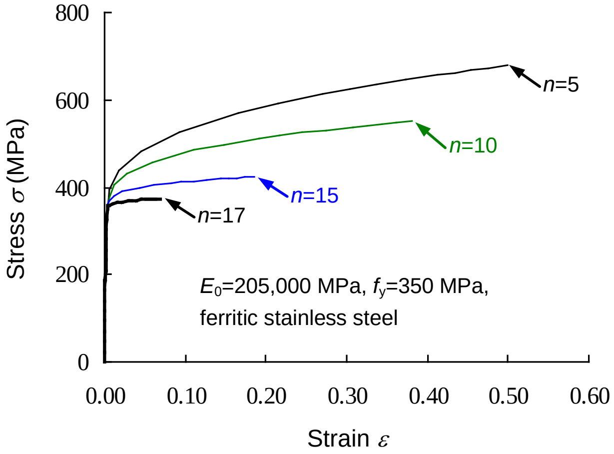

Fig. 2. Sensitivity of *n*-values on predicted σ–ε curves using Rasmussen's model

In general, Rasmussen's model is not sufficiently accurate in predicting σ–ε curves for ferritic stainless steels in most cases. A typical comparison between the predicted and measured σ–ε curves is shown in Fig. 3 for a specimen with a relatively high *n*-value of 15.8 and another specimen with a relatively high f_y of 499 MPa. When *n* is high, a conservative prediction is obtained. But the strength is overpredicted if this model is used for a material with a high f_y. It infers that some suitable modifications need to be made to improve the prediction accuracy of Rasmussen's model for ferritic stainless steels.

STRESS–STRAIN MODEL FOR FLAT MATERIAL

If Eq. (2) continues to be used for predicting σ–ε curves of ferritic stainless steels, suitable modifications to Eqs. (4)-(6) may be required in determining *m*, f_u and ε_u. For flat ferritic material, data analysis indicates that the ratio of f_u/f_y is mainly related to f_y/E_0 as shown in Fig. 4. Initially, f_u/f_y decreases with increasing f_y/E_0. But once f_y/E_0 is greater than a value of about 0.002, f_u/f_y remains almost constant. Meanwhile, no correlation is found between f_u/f_y and *n*. Based on regression analysis, the following equation is proposed to predict f_u from f_y/E_0 for ferritic stainless steels:

$$\frac{f_y}{f_u} = \begin{cases} 0.104 + 360\dfrac{f_y}{E_0} & 0.00125 \le f_y / E_0 \le 0.00235 \\ 0.95 & 0.00235 < f_y / E_0 \le 0.00275 \end{cases} \quad (7)$$

Using the above equation, the mean value and standard deviation for the ratios of tested to predicted values of f_u are 1.014 and 0.077, respectively. In contrast, the corresponding mean value and standard deviation are 0.907 and 0.226, respectively, if Eq. (5) is used instead. It should also be noted that the data points shown in Fig. 4 are not obviously biased towards a particular ferritic grade in using Eq. (7) for predicting f_u.

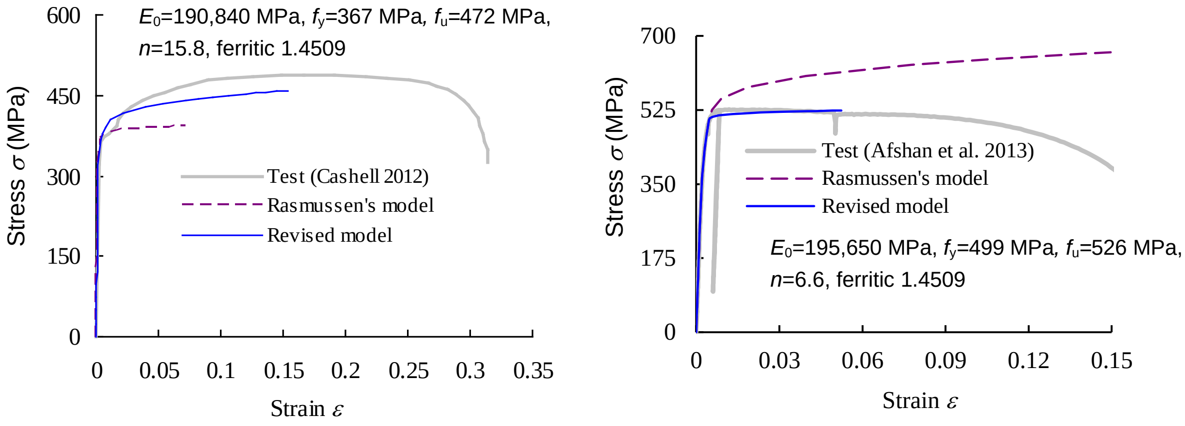

(a) (b)

Fig. 3. Evaluation of Rasmussen's model in predicting $\sigma - \varepsilon$ curves for ferritic stainless steels

Figure 5 shows the relation between ε_u and f_y/f_u. It is found that Eq. (6) proposed by Rasmussen (2003) tends to overpredict ε_u for ferritic stainless steels as demonstrated in Fig. 5. Instead, the following equation is proposed to predict ε_u for ferritic stainless steels:

$$\varepsilon_u = 0.2 - 0.2\left(\frac{f_y}{f_u}\right)^{5.5} \quad \text{for ferritic flat material} \quad (8)$$

Using this equation, the mean value and standard deviation for the ratios of tested to predicted values of ε_u are 0.962 and 0.235, respectively. If Eq. (6) is used, the corresponding mean value and standard deviation are 0.592 and 0.177, respectively.

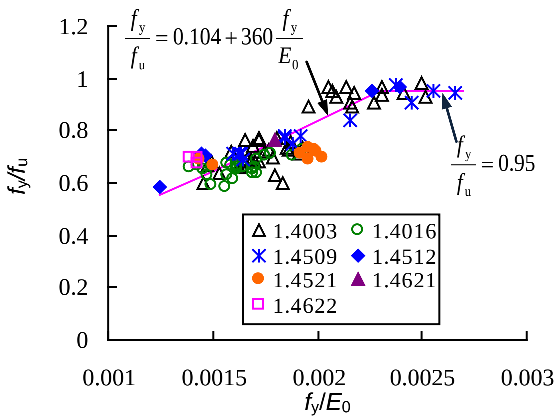

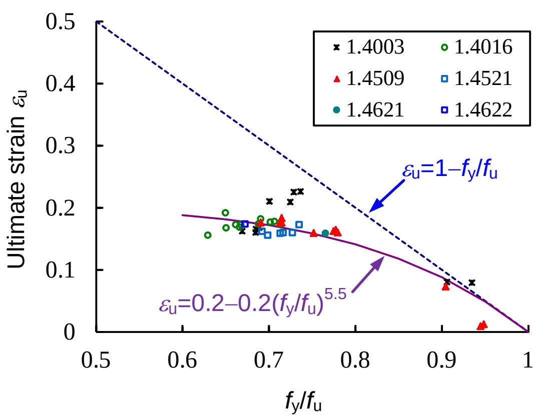

Fig. 4. Ratio of f_y/f_u as a function of f_y/E_0

Fig. 5. The relation between ε_u and f_y/f_u

In Rasmussen's model, *m* defined by Eq. (4) affects the curve shape in the stress range between the yield stress and the ultimate tensile strength, as shown in Fig. 6. In the beginning of the second stage, the strength increase is much faster with an increase in *m*. Eq. (4) was originally proposed by Rasmussen (2003) based on the trial and error method to fit measured stress-strain curves. It is found that there is no need to revise Eq. (4) for ferritic stainless steels in predicting the 35 measured σ–ε curves for flat material.

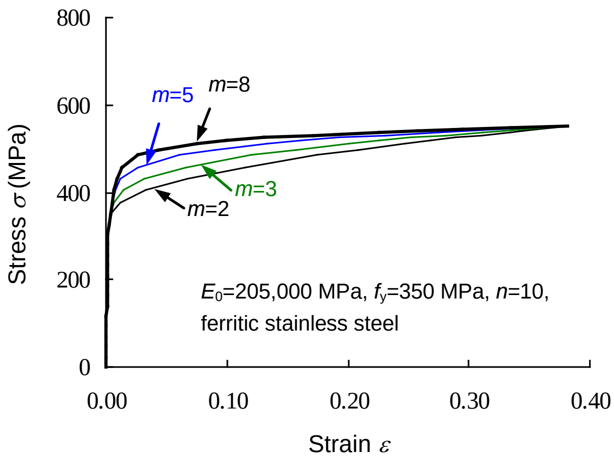

Fig. 6. Sensitivity of *m*-values on predicted σ–ε curves using Rasmussen's model

From this study, it can be concluded that Rasmussen's model can still be used for flat ferritic stainless steels, provided that Eqs. (5) and (6) are replaced by Eqs. (7) and (8), respectively. The prediction accuracy using the revised model is generally good, which is further confirmed by the comparison between predicted σ–ε curves and the collected 35 σ–ε curves. Due to the page limit, only 8 test curves from different sources are selected to illustrate the comparison shown in Figs 3 and 7. It should be noted that the test curve shown in Fig. 7(d) is converted from the true stress–strain curve reported by Rossi (2008).

STRESS–STRAIN MODEL FOR CORNER MATERIAL

Due to the combined effects of the deformation-induced dislocations and martensitic phase transformation, austenitic stainless steels demonstrate significant strength enhancement at corner regions of cold-formed sections. But the deformation hardening is less significant for duplex and ferritic stainless steels due to the lack of martensite transformation in the alloys (Hedström 2007). Compared with the flat material, an increase in both the yield stress $f_{y,c}$ and ultimate strength $f_{u,c}$ as well as a decrease in the ultimate strain $\varepsilon_{u,c}$ can be observed for the corner material of cold-formed hollow sections. The subscript "c" in the parameters $f_{y,c}$, $f_{u,c}$ and $\varepsilon_{u,c}$ indicates that these are parameters for the corner material.

Since the utilisation of the increase in mechanical properties for the corner parts of cold-formed steel sections are allowed in many design codes, the corner effects should be predicted with adequate accuracy. It will be desirable to have accurate σ–ε models for corner material, which can be used for structural analysis and design. For this purpose, Wang et al. (2014) recently proposed a σ–ε model for the material in corner regions of cold-formed hollow sections fabricated from austenitic or duplex stainless steel. This model is also a revised version of Rasmussen's σ–ε model, and expressed as:

$$\varepsilon = \begin{cases} \dfrac{\sigma}{E_0} + 0.002\left(\dfrac{\sigma}{f_{y,c}}\right)^{n_c} & \text{for} \quad \sigma \le f_{y,c} \\ 0.002 + \dfrac{f_{y,c}}{E_0} + \dfrac{\sigma - f_{y,c}}{E_{y,c}} + \varepsilon_{u,c}\left(\dfrac{\sigma - f_{y,c}}{f_{u,c} - f_{y,c}}\right)^{m_c} & \text{for} \quad f_{y,c} < \sigma \le f_{u,c} \end{cases} \tag{9}$$

where E_0 is the elastic modulus of the corresponding flat material; $f_{y,c}$ and $f_{u,c}$ are the yield stress and ultimate strength of the corner material, respectively; $\varepsilon_{u,c}$ is the ultimate strain corresponding to $f_{u,c}$; m_c is a material parameter and n_c is the strain hardening exponent; and $E_{y,c}$ is the tangent modulus of the σ–ε curve of the corner material at $f_{y,c}$, which is determined by Eq. (10). Based on data analysis of 85 tests and 24 full-range σ–ε curves, Eqs. (11)-(15) were proposed by Wang et al. (2014) to predict $f_{y,c}$, $f_{u,c}$, $\varepsilon_{u,c}$, n_c and m_c for austenitic and duplex stainless steels, respectively, where f_y, f_u, n and m in these equations are the corresponding parameters for the flat material. It should be noted that no obvious influence of cold-forming was found on the

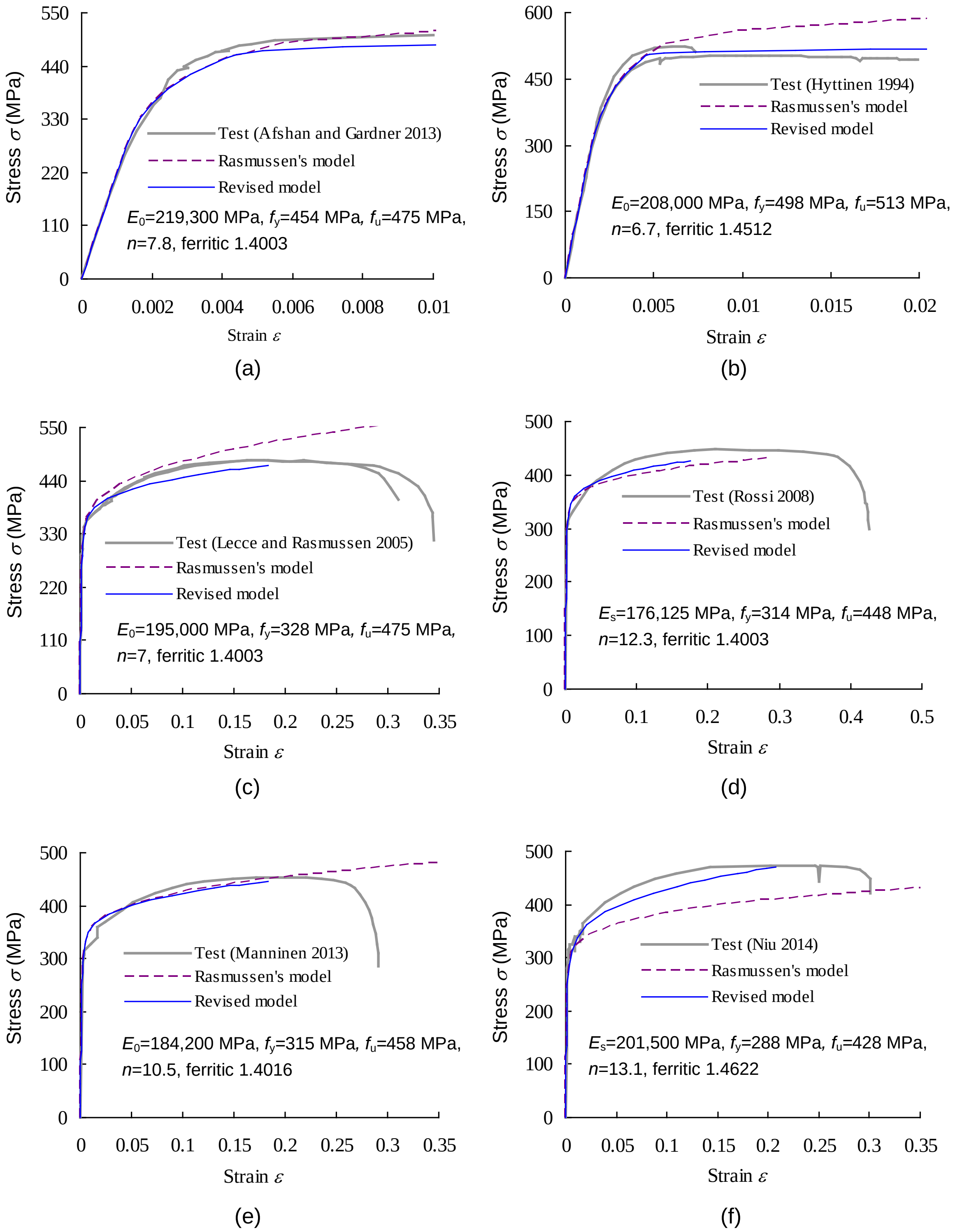

Fig. 7. Comparison between predicted and measured σ–ε curves for flat ferritic stainless steels

elastic modulus $E_{0,c}$ of corner material, and $E_{0,c}$ was taken as E_0 of the flat material in Eq. (9). This is also true for ferritic stainless steels based on the statistical analysis.

$$E_{y,c} = \frac{E_0}{1 + 0.002 n_c E_0 / f_{y,c}} \tag{10}$$

$$\frac{f_{y,c}}{f_y} = 1 + 0.05 e^{900/f_y} \tag{11}$$

$$\frac{f_{u,c}}{f_{y,c}} = \left(0.56 f_y^{\ 0.226} - 1.4\right)\frac{f_u}{f_y} \quad (12)$$

$$\varepsilon_{u,c} = 1 - \frac{f_{y,c}}{f_{u,c}} \quad (13)$$

$$n_c = 0.9 n^2 e^{-0.3n} \quad (14)$$

$$m_c = 0.04 f_y - 8 \geq m \quad (15)$$

Since the above model was specifically proposed by Wang et al. (2014) for austenitic and duplex stainless steels, it should not be expected to be suitable for ferritic stainless steels. Indeed, it can be seen from the comparison shown in Fig. 8, that the strength is greatly overpredicted by Wang et al.'s model for ferritic stainless steel alloys.

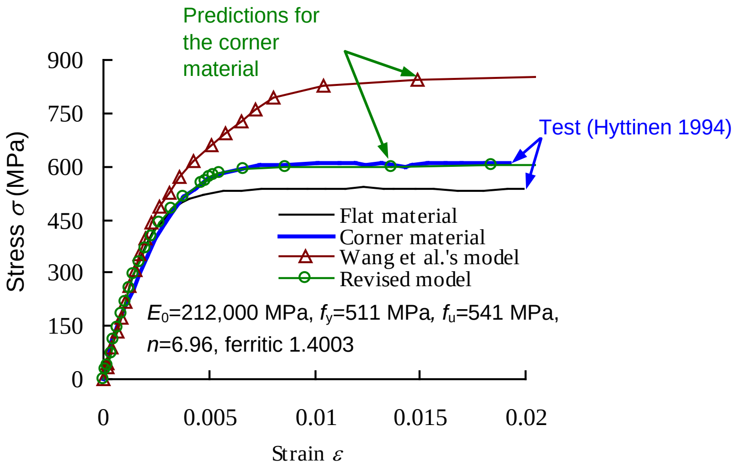

Fig. 8. Influence of cold-forming on σ–ε curves of ferritic stainless steel

As mentioned earlier, less deformation-induced strength enhancement is observed for ferritic stainless steels than austenitic or duplex stainless steels. But the strength enhancement of ferritic stainless steels shown in Fig. 8 may still be considered and utilised. In general, the σ–ε curves of ferritic corner material maintain the same basic shape of the "roundhouse" type as observed for ferritic flat material, as illustrated in Fig. 8. Therefore, suitable modifications may be made to Wang et al.'s model (Wang et al. 2014) for ferritic stainless steels in corner regions of cold-formed hollow sections.

Based on the limited test data summarised in Table 2 for ferritic stainless steels, it is found that new equations need to be developed to replace Eqs. (11) and (12), whereas the other equations proposed by Wang et al. (2014) can continue to be used for ferritic corner material. Based on regression analyses, Eqs. (16) and (17) are proposed to predict $f_{y,c}$ and $f_{u,c}$, respectively, for ferritic stainless steels. In using the two equations, $f_{y,c}$ and $f_{u,c}$ for ferritic corner material are only functions of the yield stress f_y of the corresponding flat material, since f_u can also be determined from f_y using Eq. (7). Consequently, the complete full-range tensile stress-strain curve for corner material of ferritic stainless steel alloys can be obtained from the three basic Ramberg-Osgood parameters E_0, f_y and n. The prediction accuracy of Eqs. (16) and (17) is shown in Figs 9 and 10, where the test data from (Hyttinen 1994; Afshan and Gardner 2013; Afshan et al. 2013) is shown as open circles in these figures. As can be seen, the predictions agree with the test results very well.

$$\frac{f_{y,c}}{f_y} = 0.25 + \frac{E_0}{500 f_y} \geq 1 \qquad \text{for ferritic corner material} \quad (16)$$

$$\frac{f_{u,c}}{f_{y,c}} = \left(1.55 - \frac{E_0}{840 f_y}\right)\frac{f_u}{f_y} \qquad \text{for ferritic corner material} \quad (17)$$

It is noted that m_c represented by Eq. (15) is a function of f_y. To make m_c dimension independent, Eq.(15) may be replaced by Eq. (18) to calculate m_c if f_y is nondimensionised by E_0.

$$m_c = 8000 f_y / E_0 - 8 \geq m \quad (18)$$

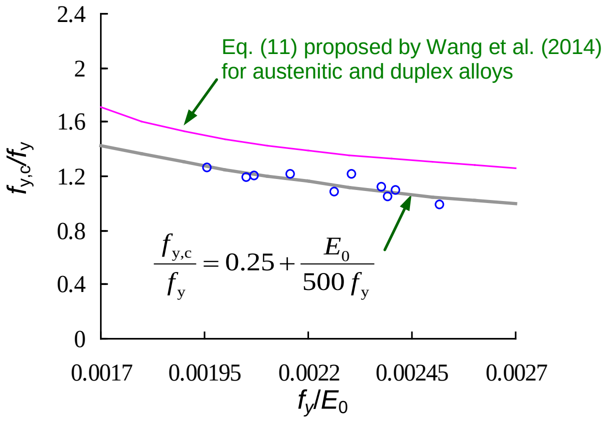

Fig. 9. The relation between $f_{y,c}/f_y$ and f_y/E_0

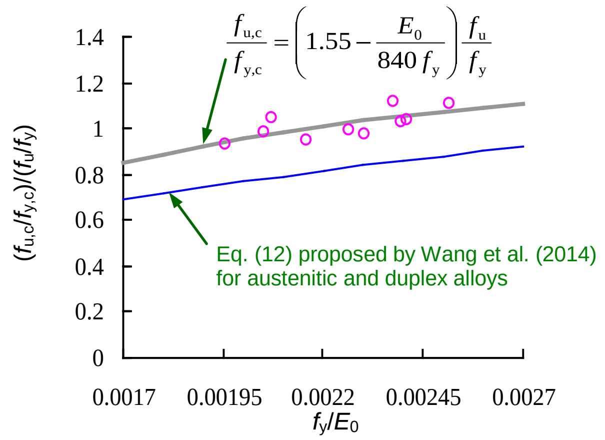

Fig. 10. Ratio of $(f_{u,c}/f_{y,c})/(f_u/f_y)$ as a function of f_y/E_0

The ten σ–ε curves tested by Hyttinen (1994), Afshan and Gardner (2013) and Afshan et al. (2013) are used to further verify the preceding revised model. Reasonably good agreement is achieved between the predictions and measured σ–ε curves, as shown in Figs 8 and 11. It is worth noting that test data for ferritic corner material is still very scarce and the existing tests only measured strains up to 0.02. More tests for corner material need to be carried out in the future to further verify this revised model.

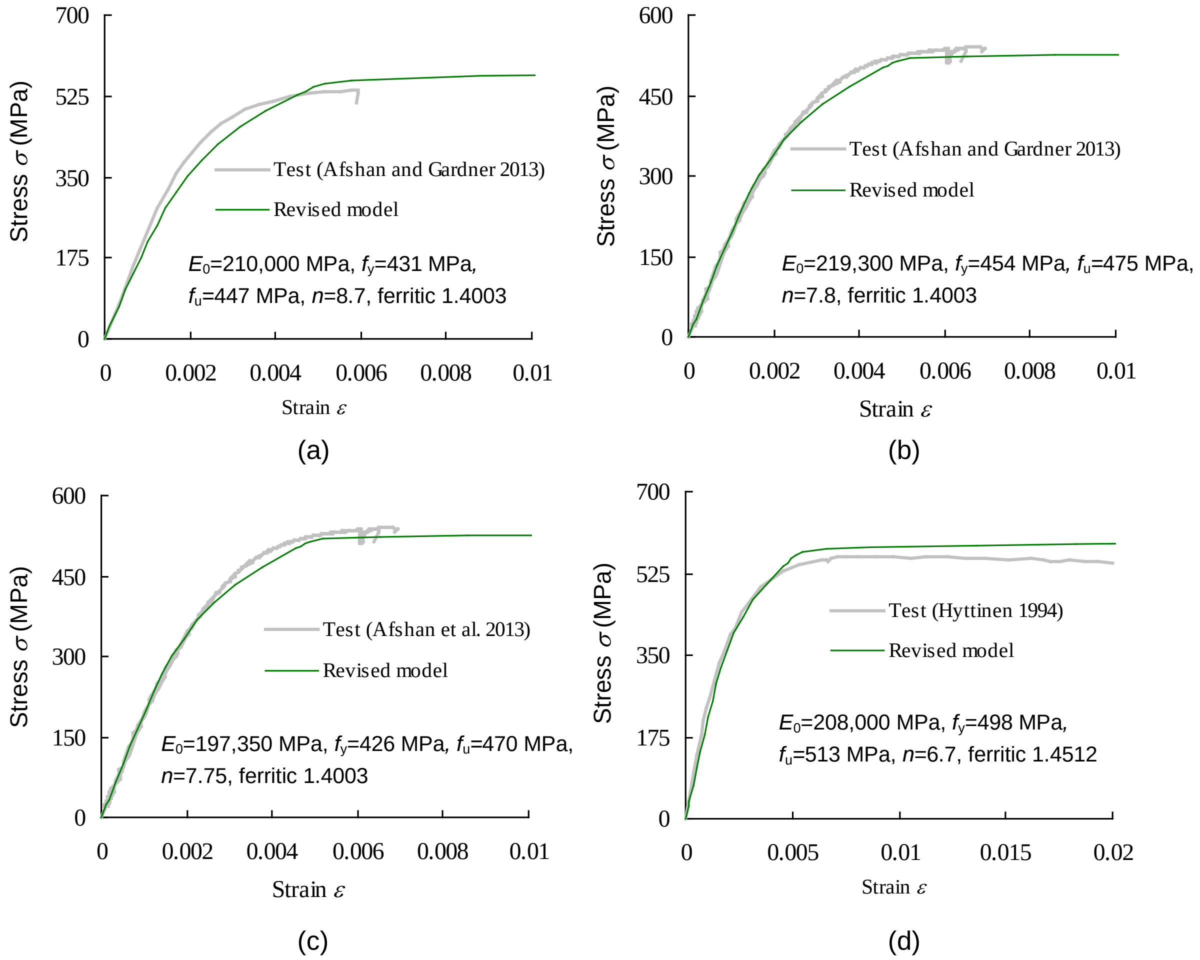

Fig. 11. Comparison between predicted and measured σ–ε curves for ferritic corner material

CONCLUSIONS

Ferritic stainless steels have different mechanical properties compared with austenitic and duplex stainless steels. Existing stress–strain models are not suitable to be used for ferritic stainless steels. Based on the models proposed by Rasmussen (2003) and Wang et al. (2014), revised models have been developed for flat material and material in corners of cold-formed ferritic stainless steel hollow sections. Only the three Ramberg-Osgood parameters of the flat material, i.e., E_0, f_y, n, are required to determine the full-range stress–strain curves. In general, the predicted stress–strain curves are in good agreement with test results. The models are valid to be used for ferritic stainless steels in tension with a yield stress ranging from 250 MPa to 550 MPa.

ACKNOWLEDGEMENTS

This work is supported by the Australian Research Council (ARC) under its Future Fellowships Scheme (Project No: FT0991433). It has also been partially supported by the ARC Discovery Project (Grant No: DP120100971). This support is gratefully acknowledged. The first author also wishes to thank Prof. L. Gardner and Dr. S. Afshan for providing their test data.

REFERENCES

Afshan, S., and Gardner, L. (2013). “Experimental study of cold-formed ferritic stainless steel hollow sections.” *Journal of Structural Engineering*, 139(5), 717–728.

Afshan, S., Rossi, B., and Gardner, L. (2013). “Strength enhancements in cold-formed structural sections—Part I: Material testing.” *Journal of Constructional Steel Research*, 83, 177–188.

Arrayago, I., Real, E., and Mirambell, E. (2013). “Constitutive equations for stainless steels: experimental tests and new proposal.” *Proceedings of the Fifth International Conference on Structural Engineering, Mechanics and Computation*, Cape Town, South Africa, 1435–1440.

ASTM International. (2012). *Metals and alloys in the Unified Numbering System* (12th Edition), Joint publication of ASTM International and SAE International, Pensylvania, USA.

Becque, J., and Rasmussen, K. J. R. (2009a). “Experimental investigation of local-overall interaction buckling of stainless steel lipped channel columns.” *Journal of Constructional Steel Research*, 65(8), 1677–1684.

Becque, J., and Rasmussen, K. J. R. (2009b). “Experimental investigation of the interaction of local and overall buckling of stainless steel I-columns.” *Journal of Structural Engineering*, 135(11), 1340–1348.

Bredenkamp, P. J., and Van den Berg, G. J. (1995). “The strength of stainless steel built-up I-section columns.” *Journal of Constructional Steel Research*, 34(2), 131–144.

Cashell, K. (2012). “Structural applications of ferritic stainless steels.” *The 4th International Experts Seminar on Stainless Steel in Structures*, Ascot, UK.

Dundu, M., and van Tonder, P. (2014). “Local buckling strength of stainless steel beam webs subjected to a stress gradient.” *Thin-Walled Structures*, 77, 48–55.

European committee for standardization. (2005). “Stainless steels–Part 1: List of stainless steels.” *EN 10088-1:2005*, Brussels, Belgium.

European committee for standardization. (2006). “Design of steel structures, Part 1–4: General rules-supplementary rules for stainless steel.” *Eurocode 3*, *EN 1993-1-4:2006*, Brussels, Belgium.

Gardner, L. (2008). “Aesthetics, economics and design of stainless steel structures.” *Advanced Steel Construction*, 4(2), 113–122.

Gardner, L., and Nethercot, D. A. (2004). “Experiments on stainless steel hollow sections—part 1: material and cross-sectional behaviour.” *Journal of Constructional Steel Research*, 60(9), 1291–1318.

Hedström, P. (2007). “Deformation and martensitic phase transformation in stainless steels.” Ph.D. thesis, Department of Applied Physics and Mechanical Engineering, Luleå University of Technology, Luleå, Sweden.

Hyttinen, V. (1994). "Design of cold-formed stainless steel SHS beam-columns." *Research Report 41*, University of Oulu, Oulu, Finland.

Islam, S. M., and Young, B. (2012). "Ferritic stainless steel tubular members strengthened with high modulus CFRP plate subjected to web crippling." *Journal of Constructional Steel Research*, 77, 107–118.

Korvink, S. A., Van den Berg, G. J., and Van der Merwe, P. (1995). "Web crippling of stainless steel cold-formed beams." *Journal of Constructional Steel Research*, 34(2), 225–248.

Lecce, M., and Rasmussen, K. J. R. (2005). "Experimental investigation of the distortional buckling of cold-formed stainless steel sections." *Research Report No. R844*, Department of Civil Engineering, the University of Sydney, Sydney, Australia.

Lim, J. S., Kim, T. S., and Kim, S. H. (2013). "Ultimate strength of single shear bolted connections with cold-formed ferritic stainless steel." *Journal of Zhejiang University: Science A*, 14(2), 120–136.

Manninen, T. (2013). "WP1.3: Characterization of stress-strain behaviour. RFCS Project 'Structural application of ferritic stainless steels'." *Contract no. RFSR-CT-2010-00026*, Outokumpu Stainless Oy, Tornio, Finland.

McGuire, M. F. (2008). *Stainless steels for design engineers*, ASM International, Materials Park, Ohio, USA.

Niu, S., Rasmussen, K. J. R, and Fan, F. (2014). "Distortional–global interaction buckling of stainless steel C-beams: Part I—Experimental investigation." *Journal of Constructional Steel Research*, 96, 127–139.

Oliphant, Q. C., van den Berg, G. J., and van Tonder, P. (2000). "Eccentrically loaded bolted connections for type 304 and 3Cr12 stainless steel lipped channels." *Proceedings of the Fifteenth International Specialty Conference on Cold-formed Steel Structures*, St. Louis, Missouri, USA, 715–726.

Quach, W. M., Teng, J. G., and Chung, K. F. (2008). "Three-stage full-range stress–strain model for stainless steels." *Journal of Structural Engineering*, 134(9), 1518–1527.

Rasmussen, K. J. R. (2001). "Full-range stress–strain curves for stainless steel alloys." *Research Report No. R811*, Department of Civil Engineering, University of Sydney, Sydney, Australia.

Rasmussen, K. J. R. (2003). "Full-range stress–strain curves for stainless steel alloys." *Journal of Constructional Steel Research*, 59(1), 47–61.

Real, E., Arrayago, I., Mirambell, E., and Westeel, R. (2012). "Comparative study of analytical expressions for the modeling of stainless steel behaviour." *The 4th International Experts Seminar on Stainless Steel in Structures*, Ascot, UK.

Rossi, B. (2008). "Mechanical properties, residual stresses and structural behavior of thin-walled stainless steel profiles." Ph.D. thesis, Faculty of Applied Sciences, University of Liège, Liège, Belgium.

Rossi, B., Franssen, J. M., and Tondini, N. (2013). "Experiments on ferritic stainless steel columns in fire." *Proceedings of the Fifth International Conference on Structural Engineering, Mechanics and Computation*, Cape Town, South Africa, 1465–1470.

Tao, Z., Uy, B., Liao, F. Y., and Han, L. H. (2011). "Nonlinear analysis of concrete-filled square stainless steel stub columns under axial compression." *Journal of Constructional Steel Research*, 67(11), 1719–1732.

Uy, B., Tao, Z., and Han, L. H. (2011). "Behaviour of short and slender concrete-filled stainless steel tubular columns." *Journal of Constructional Steel Research*, 67(3), 484–496.

Van der Merwe, P., and van den Berg, G. J. (1987). "Experimental stress-strain curves for cold-rolled type 430 steel sheets." *Internal Report no. MD-36*, Department of Civil Engineering, Rand Afrikaans University, Johannesburg, South African.

Van der Merwe, P., van den Berg, G. J., and Marshall, V. (1986). "Experimental stress-strain curves for cold-rolled 3Cr12 steel sheets." *Internal Report no. MD-21*, Department of Civil Engineering, Rand Afrikaans University, Johannesburg, South African.

Wang, X. Q., Tao, Z., Song, T. Y., and Han, L. H. (2014). "Stress-strain model of austenitic stainless steel after exposure to elevated temperatures." *Journal of Constructional Steel Research*, 99, 129–139.